APPENDIX

A. MESHING OF MODELS DURING CFD ANALYSIS

A.0.1. Conformal Meshing. The conformal meshing style creates the object mesh globally. Hence, small objects unnecessarily increase the mesh complexity of larger objects around them.

A.0.2. Non-conformal Meshing. Non-conformal meshing allows us to specify local meshing parameters for each object. Hence, meshing is done for each object separately. In other words, it localizes the mesh density. Figures 16 to 18 show the mesh generated during CFD analysis for the various models.

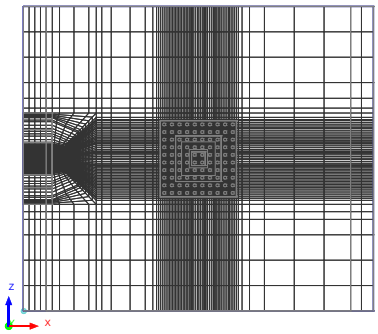

Fig. 16. Conformal mesh for a sever

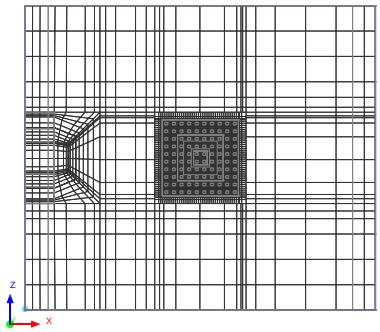

Fig. 17. Non-conformal mesh for a sever

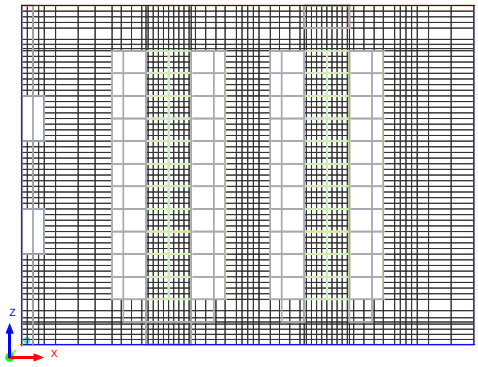

Fig. 18. Data center mesh created using non-conformal meshing

B. SPL PROFILE OF THE DATA CENTER FOR SCENARIO I

Figures 19–30 show the SPL distribution for different for scenario I.

In all the three scenarios, for all the cases, maximum temperature during simulation never exceeds the threshold temperature. In Appendix D, Figures 41 to 49 show temperature profile inside the data center for uniform workload distribution, heuristic-I and heuristic-II for scenario-I. For other scenarios also the maximum temperature inside the data center is around $30\,^{\circ}\mathrm{C}$.

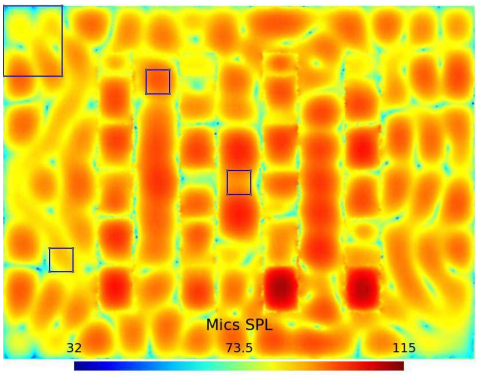

Fig. 19. SPL distribution on microphones plane for uniform workload distribution for scenario-I

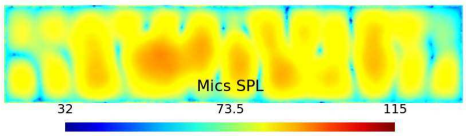

Fig. 20. SPL distribution on the datacenter wall for uniform distribution for scenario-I

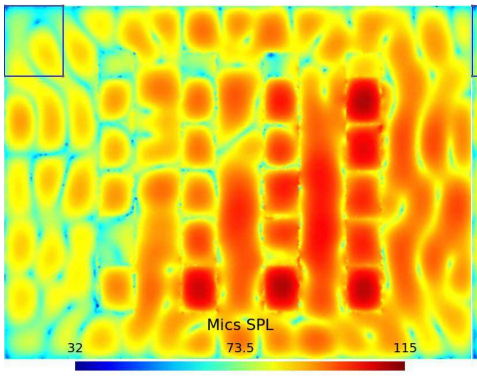

Fig. 21. SPL distribution on microphones after workload redistribution for corner office with heuristic-I for scenario-I

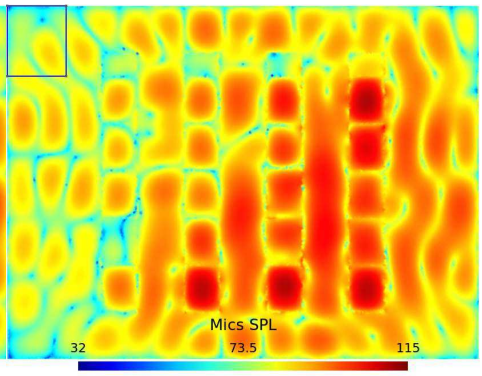

Fig. 22. SPL distribution on microphones after workload redistribution for corner office with heuristic-II for scenario-I

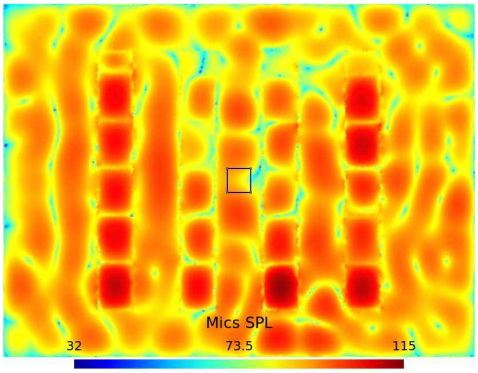

Fig. 23. SPL distribution on microphones after workload redistribution for worker with heuristic-I for scenario-I

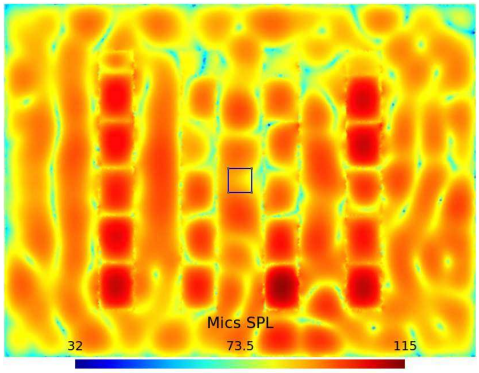

Fig. 24. SPL distribution on microphones after workload redistribution for worker with heuristic-II for scenario-I

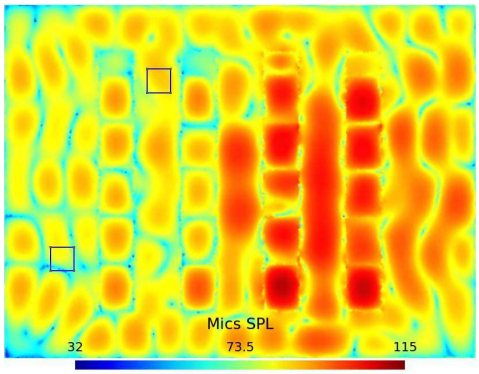

Fig. 25. SPL distribution on microphones after workload redistribution for multiple workers with heuristic-I for scenario-I

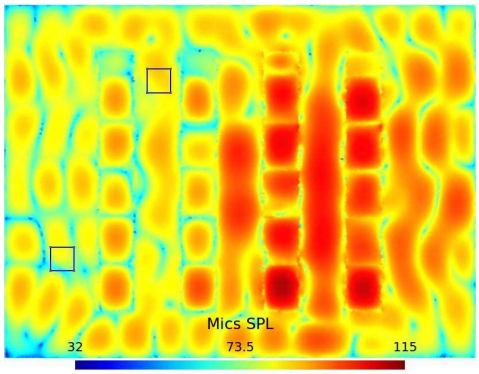

Fig. 26. SPL distribution on microphones after workload redistribution for multiple workers with heuristic-II for scenario-I

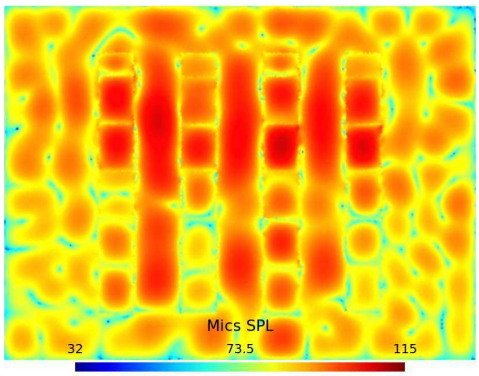

Fig. 27. SPL distribution on microphones after workload redistribution for side wall with heuristic-I for scenario-I

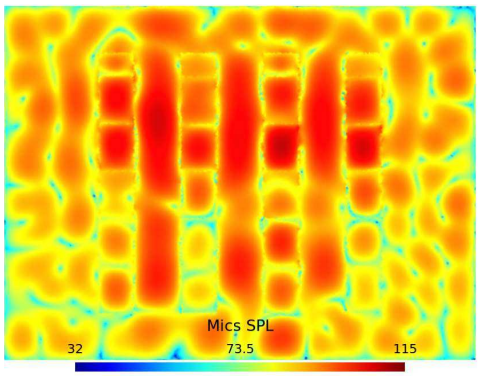

Fig. 28. SPL distribution on microphones after workload redistribution for side wall with heuristic-II for scenario-I

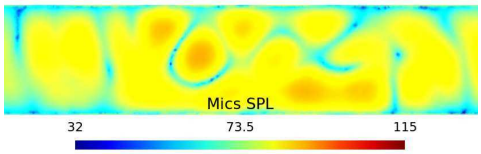

Fig. 29. SPL distribution on the datacenter wall for heuristic-I for scenario-I

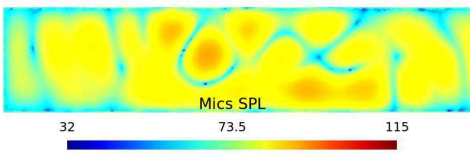

Fig. 30. SPL distribution on the datacenter wall for heuristic-II for scenario-I

C. SPL PROFILE OF THE DATA CENTER FOR SCENARIO-II

For heuristic-II, the SPL profiles obtained are shown in Figures 31-40 for various locations of interest.

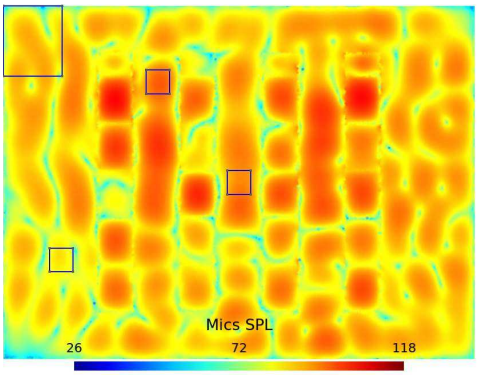

Fig. 31. SPL distribution on microphones plane for uniform workload distribution for scenario-II

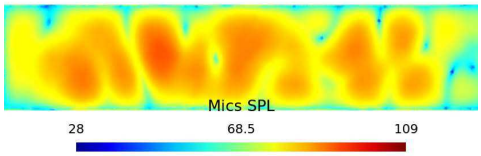

Fig. 32. SPL distribution on the datacenter wall for uniform distribution for scenario-II

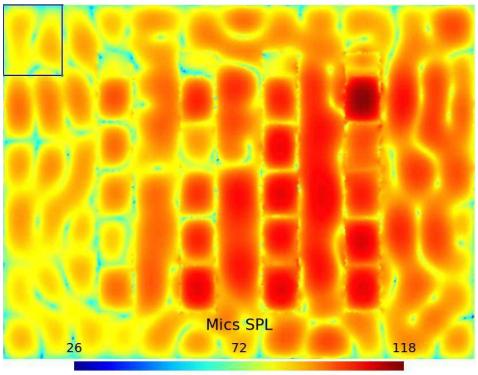

Fig. 33. SPL distribution on microphones after workload redistribution for corner office with heuristic-I for scenario-II

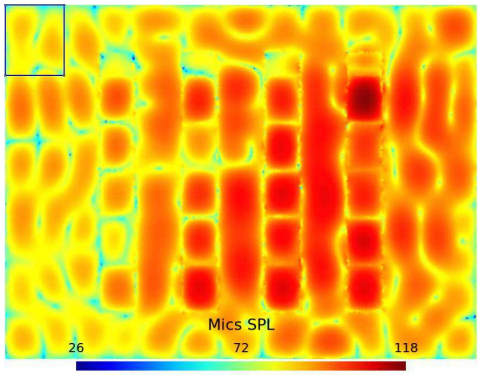

Fig. 34. SPL distribution on microphones after workload redistribution for corner office with heuristic-II for scenario-II

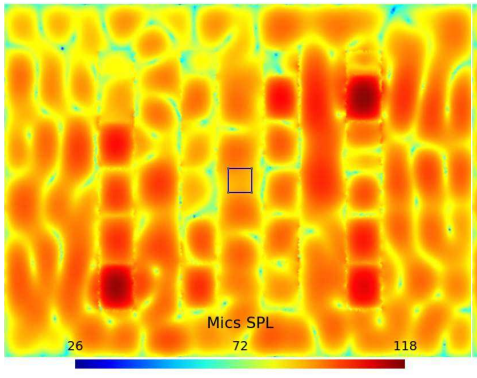

Fig. 35. SPL distribution on microphones after workload redistribution for worker with heuristic-I for scenario-II

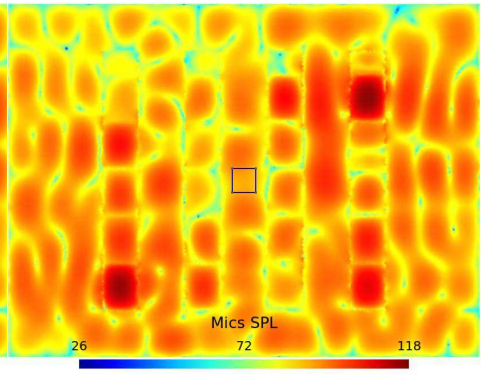

Fig. 36. SPL distribution on microphones after workload redistribution for worker with heuristic-II for scenario-II

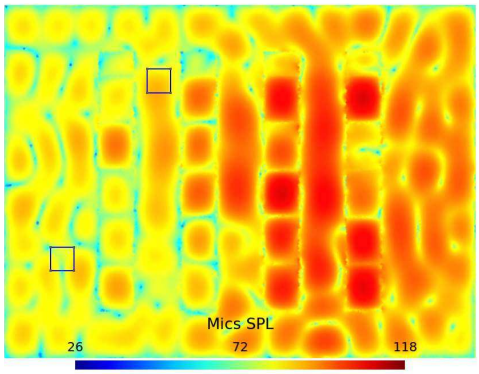

Fig. 37. SPL distribution on microphones after workload redistribution for multiple workers with heuristic-I for scenario-II

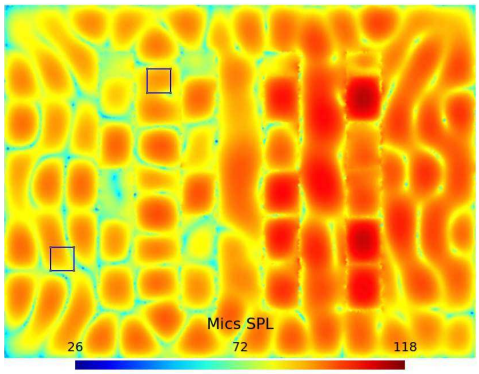

Fig. 38. SPL distribution on microphones after workload redistribution for multiple workers with heuristic-II for scenario-II

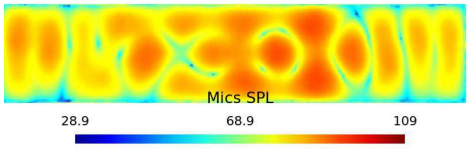

Fig. 39. SPL distribution on the datacenter wall with heuristic-I for scenario-II

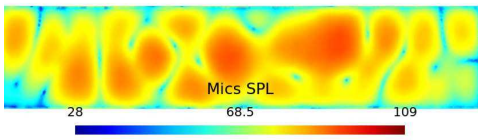

Fig. 40. SPL distribution on the datacenter wall with heuristic-II for scenario-II

D. THERMAL PROFILE OF THE DATA CENTER

The temperature diagrams below (Figures 41 to 45) show how the thermal profile inside the data center changes for scenario-I as we consider various locations for noise reduction.

E. POWER CONSUMPTION FOR DIFFERENT BENCHMARKS

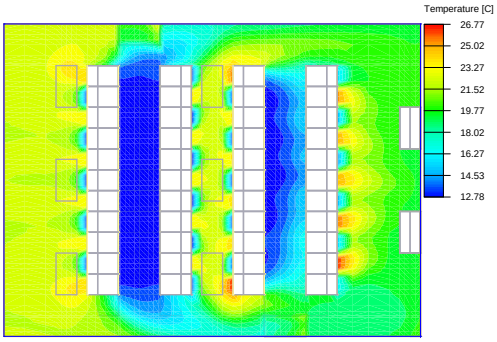

Fig. 41. Temperature profile inside data center for uniform workload distribution

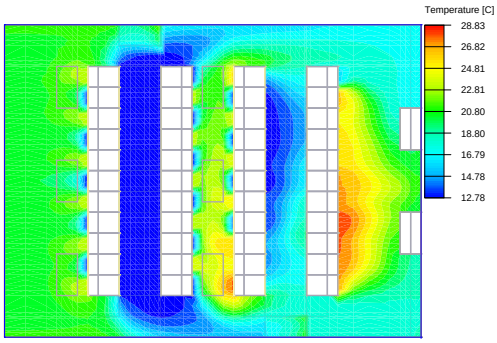

Fig. 42. Temperature profile inside data center after workload distribution for corner office with heuristic-I

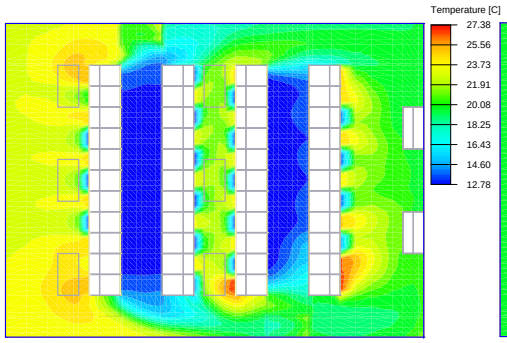

Fig. 43. Temperature profile inside data center after workload distribution for single worker with heuristic-I

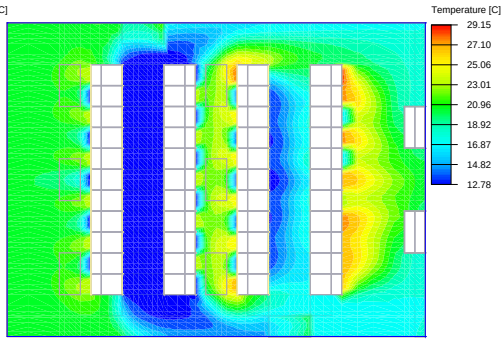

Fig. 44. Temperature profile inside data center after workload distribution for multiple workers with heuristic-I

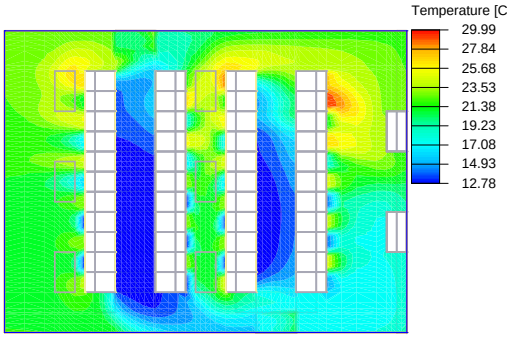

Fig. 45. Temperature profile inside data center after workload distribution for side wall with heuristic-I

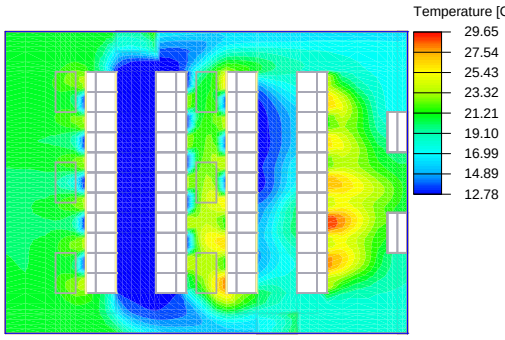

Fig. 46. Temperature profile inside data center after workload distribution for corner office with heuristic-II

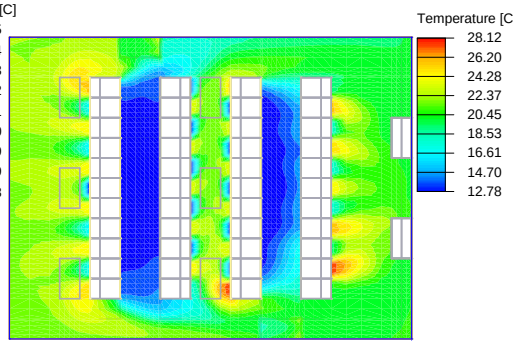

Fig. 47. Temperature profile inside data center after workload distribution for single worker with heuristic-II

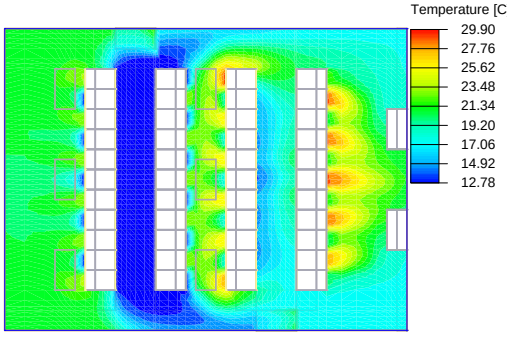

Fig. 48. Temperature profile inside data center after workload distribution for multiple workers with heuristic-II

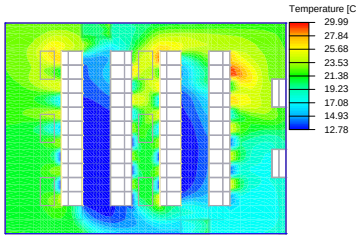

Fig. 49. Temperature profile inside data center after workload distribution for side wall with heuristic-II

Table X. Parsec benchmarks with their measured power consumption

Combination of Parsec benchmarks run on a single server	Measured Power Consumption ($Watt$)
Idle	98.9
blackscholes	149.5
bodytrack	144.9
ferret	124.2
freqmine	126.5
swaptions	156.4
canneal	124.2
streamcluster	135.7
blackscholes bodytrack	170.2
blackscholes ferret	138
ferret streamcluster	151.8
freqmine swaptions	163.3
freqmine swaptions	190.9
freqmine swaptionsLarge	197.8
freqmine canneal	133.4
freqmine streamcluster	154.1
swaptions swaptions	197.8
blackscholes swaptions streamcluster	193.2
blackscholes swaptions canneal	197.8
blackscholes swaptions streamcluster	195.5
bodytrack swaptions swaptions	202.4
bodytrack swaptions canneal	184.0
bodytrack swaptions streamcluster	190.9
ferret freqmine swaptions	172.5
blackscholes bodytrack freqmine streamcluster	190.9
blackscholes bodytrack swaptions canneal	197.8
blackscholes bodytrack swaptions streamcluster	195.5
bodytrack ferret swaptions canneal	190.9
bodytrack ferret swaptions streamcluster	195.5
freqmine swaptionsLarge canneal streamcluster	207.0
blackscholes ferret freqmine swaptions streamcluster	200.1
blackscholes bodytrack ferret freqmine swaptions streamcluster	202.4
blackscholes bodytrack ferret freqmine canneal streamcluster	202.4
blackscholes bodytrack ferret swaptions canneal streamcluster	195.5
blackscholes bodytrack freqmine swaptions canneal streamcluster	204.7
blackscholes ferret freqmine swaptions canneal streamcluster	200.1